Superconducting Microresonator Detectors

J. Zmuidzinas

August 9, 2008

1 Technical Description

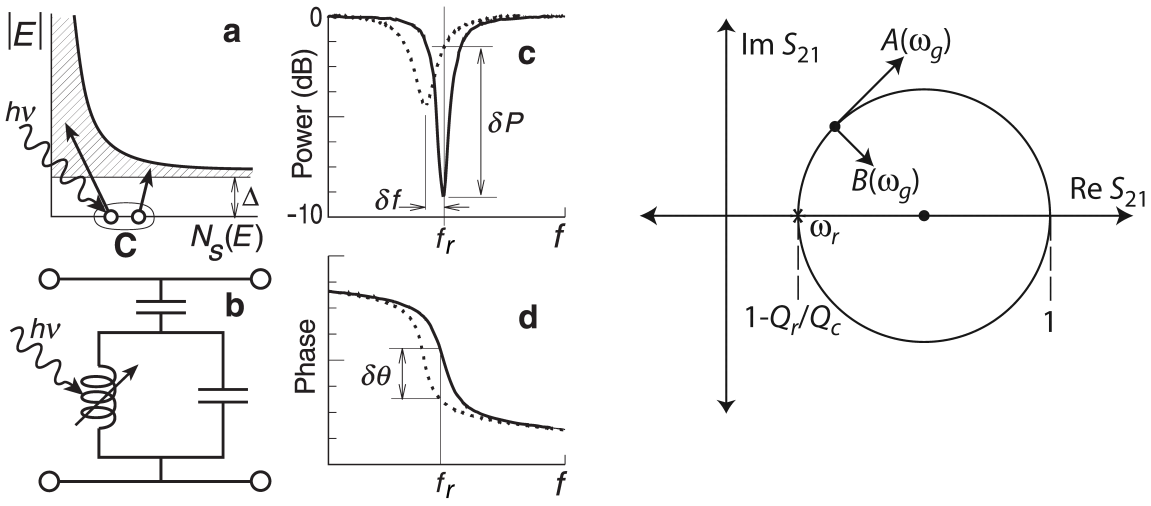

Figure 1: **Left**: Principle of operation of superconducting microresonator detectors, following[1]. The absorbed photon energy breaks Cooper electron pairs in a thin superconducting film (a) which is part of a lithographed microresonator circuit (b). The breaking of Cooper pairs causes a change in the surface reactance and resistance of the film, leading to a shift in the resonance frequency f_r and a reduction of the resonator's quality factor Q_r (c), which can be sensed by measuring the phase (d) and amplitude (c) of the microwave output signal. **Right**: This figure illustrates the trajectory of the resonator's transmission $S_{21}(\omega)$ as a function of angular frequency ω in the complex plane. The transmission is unity ($S_{21} = 1$) at frequencies away from resonance. Starting at a frequency below resonance, S_{21} traces out the circle in a clockwise direction as the frequency is increased, crossing the real axis at the resonance frequency ω_r indicated by the star, and corresponding to a transmission $S_{21}(\omega_r) = 1 - Q_r/Q_c$ as indicated, where Q_c is the coupling-limited quality factor. The adiabatic response coefficients for changes in the resonator frequency $A(\omega_g)$ and dissipation $B(\omega_g)$ are shown for the case that the generator frequency ω_g is tuned above the resonance. These coefficients are tangent to and perpendicular to the resonance circle, respectively.

1.1 Basic Physics

The basic concept of operation is described in a number of publications [1–6] and is illustrated in Fig. 1. Photons are absorbed in a superconducting film, which causes Cooper electron pairs to break. The binding

energy of Cooper pairs is proportional to the critical temperature, $2\Delta \approx 3.5 k_B T_c$, which corresponds to a minimum photon frequency $\nu = 2\Delta/h \approx 90$ GHz for aluminum ($T_c = 1.2$ K). A perturbation δP of the absorbed mm-wave power thereby produces a perturbation $\delta Z_s = \delta R_s + j\delta X_s$ of the complex microwave surface impedance of the film. Both the real and imaginary parts of the impedance are affected in this process: Cooper pair breaking causes the surface reactance to increase (this is the "kinetic inductance" effect), and meanwhile the single electrons (or "quasiparticles") that are produced are capable of scattering, and are therefore dissipative, and are responsible for an increase in the surface resistance. Both of these effects can be sensed by incorporating the superconducting film into a resonant circuit and measuring the resulting changes in the resonance frequency and quality factor, as shown in Fig. 1.

The readout of the resonator can be explained more precisely by considering the trajectory of the complex microwave transmission $S_{21}(\omega)$ in the complex plane as the angular (microwave) frequency ω is varied. The linewidth of the resonance is $\Delta\omega_r = \omega_r/Q_r$, where the resonator's quality factor is determined by coupling and internal losses according to the usual formula, $Q_r^{-1} = Q_c^{-1} + Q_i^{-1}$. Away from resonance, the transmission is essentially unity $|S_{21}| = 1$, and near resonance describes a circle with the resonance frequency being the point of closest approach to the origin, as shown in Fig. 1. If the readout generator's frequency ω_g is fixed, and a change in optical power δP is introduced, the resulting change in the surface reactance δX_s will cause a perturbation in the complex transmission δS_{21} that is tangent to the resonance circle; meanwhile, δR_s causes δS_{21} to move in a perpendicular direction. The overall response is the vector sum of these two components. Therefore, by using readout electronics that are capable of real-time vector measurements of S_{21}, one can simultaneously measure and separate these two effects. However, the perturbation in the reactance is a stronger effect: the ratio is $\delta R_s/\delta X_s \equiv \tan\psi \approx 0.3$ [6–8]; this ratio also describes the relative strengths of the transmission perturbations δS_{21} for the tangent and perpendicular directions. This is of practical importance: the factor of $\sim 3-4$ lower responsivity for the dissipation readout places more stringent demands on the noise performance of the cryogenic microwave amplifier that follows the resonator (see section 1.4).

1.2 A millimeter-wave implementation

A practical implementation of this concept for mm-wave detection is shown in Fig. 2, using a quarter-wavelength transmission-line resonator rather than a lumped-element circuit. A coplanar waveguide (CPW) transmission line allows the resonator to be made without the use of deposited dielectric films (which are amorphous and generally lossy[9]), thereby allowing extremely high quality factors ($Q_r \sim 10^6$) to be achieved. The use of an aluminum section near the shorted end of the resonator allows absorption of mm-wave radiation at freuencies above 90 GHz (a lower T_c material would be needed for frequencies below 90 GHz). The mm-wave radiation is brought to the resonator using a low-loss $Nb/SiO_2/Nb$ microstrip line which runs across the aluminum center strip of the CPW resonator, at which point it becomes a $Nb/SiO_2/Al$ microstrip, causing mm-wave dissipation and pair-breaking in the Al strip.

The use of microstrip coupling allows this type of detector to be used with a variety of feeds, including narrow-beam phased-array planar antennas [10–16] with either single or dual-polarization response, broad-beam planar antennas [17–22], and the more traditional horn-waveguide-probe coupling approaches [23–27].

Other coupling techniques are possible, and indeed necessary at frequencies above 700 GHz where niobium microstrip lines become exceedingly lossy. Coupling of far-infrared radiation into an aluminum CPW resonator directly attached to a twin-slot antenna has been demonstrated[28]. Another possibility is to design the inductive portion of the resonator to simultaneously be a good far-infrared absorber. This approach has also been demonstrated[29, 30] and leads to two-dimensional pixel arrays similar to absorber-coupled transition-edge sensor (TES) bolometer arrays. Other approaches for far-infrared microresonator detectors are also being actively pursued (E. Wollack, priv. comm.).

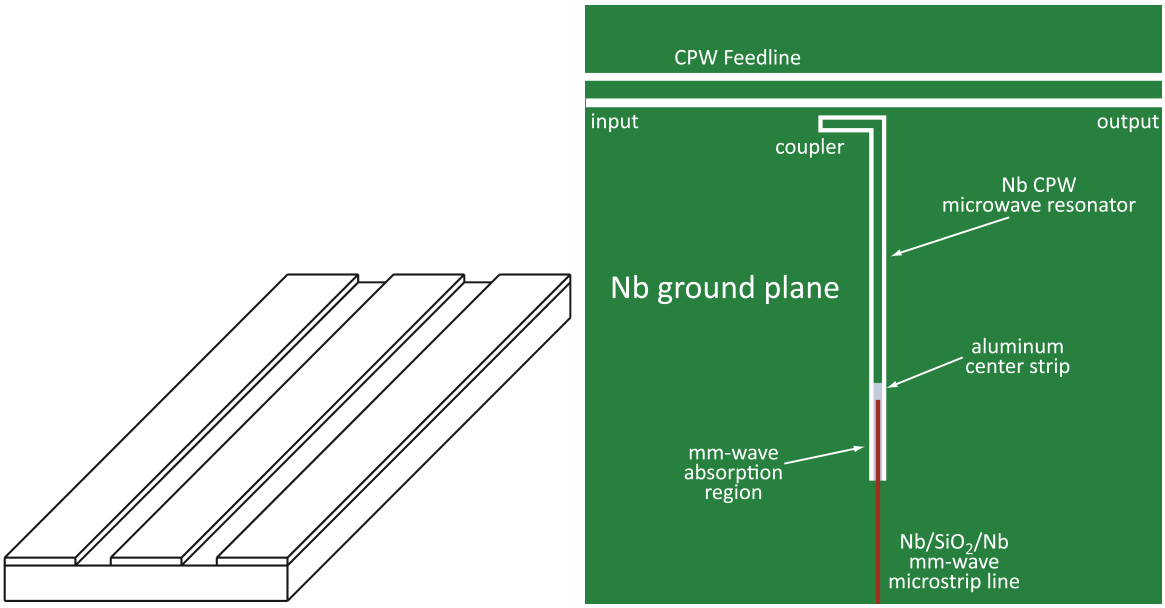

Figure 2: **Left**: A coplanar waveguide (CPW) transmission line is fabricated by etching two parallel slots in a metal film, which defines a center conductor and two ground planes. **Right**: A typical microstrip-coupled mm-wave detector made using a hybrid niobium/aluminum (Nb/Al) CPW quarter-wave resonator. The resonator is short-circuited at the bottom, where the mm-wave radiation is absorbed, and is open-circuited at the top, where the resonator is coupled to the feedline. The microwave readout signal propagates along the CPW feedline at the top, fed from the signal generator on the left and coupled to the cryogenic low-noise amplifier on the right. The readout signal excites the resonator via the coupler section; the length of the coupler and its separation from the feedline dictate the value of the coupling quality factor Q_c. At the short-circuit end, a strip of aluminum is used for the CPW resonator center strip in place of niobium, because the superconducting gap energy of aluminum allows it to absorb mm-wave radiation with frequencies above 90 GHz; the corresponding gap frequency of niobium is 700 GHz. The mm-wave radiation is coupled to the aluminum strip using a low-loss $Nb/SiO_2/Nb$ microstrip (parallel-plate) transmission line, as shown, and is absorbed over the $\sim 1\,\mathrm{mm}$ length of the aluminum strip. The typical dimensions are $6\,\mu\mathrm{m}$ for the CPW center strip width, $2\,\mu\mathrm{m}$ for the CPW slot, and ~ 5 mm for the resonator length, giving a resonance frequency around 6 GHz.

1.3 Frequency multiplexing

Because the resonators have high quality factors ($Q_r = 10^4 - 10^6$), a large number of resonators may be multiplexed in the frequency domain and read out with a single cryogenic microwave amplifier, as shown in Fig. 3. In this scheme, the resonators are coupled to a common feedline and therefore the detector chip is fully multiplexed, as opposed to TES designs which require multi-lead superconducting connections between the detector and SQUID multiplexer for each pixel (this is true for all types of SQUID multiplexing - time domain as well as MHz/GHz frequency-domain). The room-temperature electronics then has the job of generating a set of excitation frequencies - one per resonator - and then measuring the amplitudes and phases of these signals after they have been sent into the cryostat, transmitted past the resonator array, and amplified by the cryogenic amplifier and any additional room-temperature amplifiers. Fortunately, this task has become quite feasible using modern digital signal processing techniques.

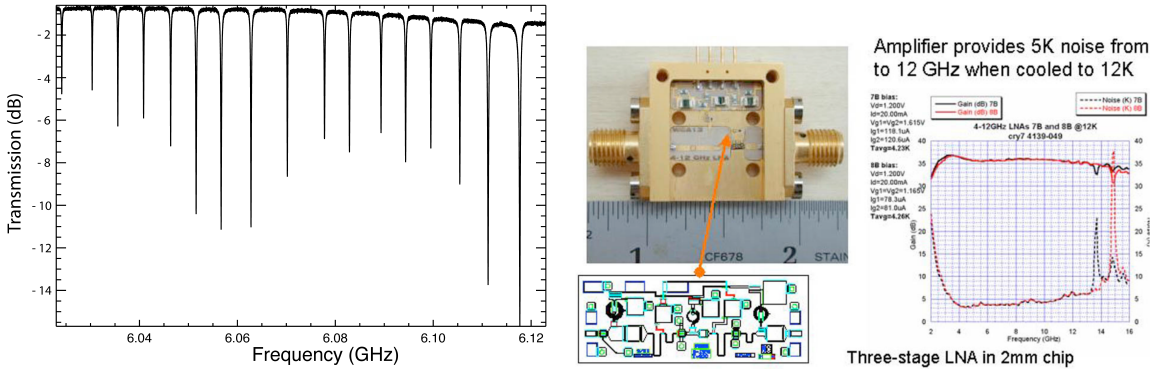

Figure 3: **Left**: an example of an array of resonators coupled to a single feedline. The depths of the resonances depend on the coupler design and the value of the coupling quality factor Q_c (credit: B. Mazin). **Right**: A single wide-band cryogenic HEMT amplifier (credit: S. Weinreb). can be used to simultaneously measure a large number ($\sim 10^3$) of resonators.

1.4 Sensitivity

1.4.1 Fundamental Limits

The fundamental sensitivity limit for this type of detector is set by the random generation of quasiparticles by pair-breaking thermal phonons, and their subsequent recombination. However, this mechanism is exponentially suppressed at low temperatures by the Boltzmann factor $\exp(-\Delta/k_B T)$ due to the superconducting energy gap, and therefore in practice the sensitivity is determined by other factors. Ideally, the sensitivity would be set by photon arrival statistics - the BLIP limit. One interesting subtlety is whether the BLIP limit for these detectors corresponds to a "photodiode" or "photoconductor" device – the latter being less sensitive by a factor of $\sqrt{2}$ due to the additional noise introduced by the random carrier lifetimes (recombination noise). The answer is "both" ! For photon energies just above the gap, $h\nu = 2\Delta + \delta E$, only a single Cooper pair is broken, and the recombination process adds significant noise, but the factor is $\sqrt{3/2} = 1.2$ instead of the full $\sqrt{2}$ because two quasiparticles must recombine. Far above the gap, $h\nu >> 2\Delta$, a large number of quasiparticles are produced, and each quasiparticle recombines randomly, so the recombination noise is averaged down to an insignificant level and "photodiode" performance is obtained.

1.4.2 Conditions for Achieving BLIP Operation

Achieving the BLIP limit requires that the amplifier noise contribution be brought below the photon noise. This requires optimizing the responsivity of the device, which in practice amounts to choosing the correct value of the coupling quality factor Q_c. For low photon backgrounds, the number of photo-produced quasiparticles will be small, and so the resonator's internal dissipation Q_i^{-1} due to the quasiparticles will also be small; conversely, for large backgrounds the dissipation will be larger, and the quality factor will be lower. The coupling strength which maximizes the responsivity is given by $Q_c = Q_i$[6, p. 77]. This design optimization is analogous to choosing the desired value of thermal conductance G for a bolometer given the expected optical loading. The second key issue for achieving BLIP is the noise performance of the cryogenic amplifier that is required for an optimized detetector ($Q_c = Q_i$). This question has been studied in some detail theoretically; the answer[6, equation (6.43)] depends on a number of factors including the gap frequency, the photon frequency, the background loading, the quasiparticle lifetime, the maximum microwave readout power, and crucially, on whether one is using frequency or dissipation readout (see the discussion in section 1.1). Calculations[6, Table 6.1] indicate that readily achievable amplifier noise temperatures in the range $T_n = 10 - 20$ K would allow BLIP operation using frequency readout, whereas much better performance ($T_n = 1 - 2$ K) is needed for dissipation readout. Because the amplifier contribution to the noise equivalent power (NEP) scales as $\sqrt{T_n}$, the use of a typical HEMT amplifier (see Fig. 3) with $T_n = 5\,\mathrm{K}$ for dissipation readout will result in an NEP value that is roughly twice the BLIP limit. Finally, although the detailed physics of quasiparticle recombination is not fully understood yet[31], the measured lifetimes are sufficiently long and do not impose a serious limitation on CMB observations.

1.4.3 Excess Frequency Noise

Although amplifier noise considerations lead one to focus on using frequency readout, it turns out that CPW microresonators suffer from excess frequency noise. This excess noise prevents the detectors from achieving BLIP performance by a factor of around $5 - 6$[6, Table 6.1] when using frequency readout. The excess noise problem was appreciated early on[1] and stimulated efforts to determine the source of the noise and its general properties. The excess frequency noise rises at low frequencies but has a relatively shallow spectrum, $\sim 1/f^{0.5}$ (see Fig. 4), which implies that the NEP varies very slowly, as $1/f^{0.25}$. The early evidence indicated that the noise did not originate in the superconducting films but rather in the substrate or its surface[4]. Therefore, by using very thin superconducting aluminum films ($t \sim 40$ nm), the frequency responsivity of the device was increased dramatically, and allowed the NEP at 1 Hz to be reduced from the $\sim 10^{-15}\,\mathrm{W}/\sqrt{\mathrm{Hz}}$ level in 2003 to $\sim 10^{-17}\,\mathrm{W}/\sqrt{\mathrm{Hz}}$ in 2005.

1.4.4 Pushing Toward BLIP Performance

Further work[7] showed that the noise really affects just the resonator frequency; no excess noise was seen in the dissipation signal above the level of the amplifier noise (see Fig. 4). This of course opens up the possibility of using the dissipation readout with very high-Q resonators in order to achieve very low NEP values, and this idea has been actively pursued by the SRON group[33, 34]. Their lowest achieved NEP to date is $7 \times 10^{-19}\,\mathrm{W}/\sqrt{\mathrm{Hz}}$ and is steadily decreasing as the quality of the devices and measurement setup are improved. Although this NEP value is actually better than required for broadband CMB measurements, the NEP will degrade as optical loading is applied because the resonator quality factor will be reduced. The conclusion is that even for CMB measurements from space, microresonator-based detectors used in dissipation readout mode can already achieve sensitivities within a factor of 2 or so from BLIP.

One approach to push closer towards the BLIP limit is to use dissipation readout with a lower-noise amplifier. Good progress is being made in this direction through the work by Weinreb and colleagues[35, 36] on cryogenic SiGe bipolar amplifiers; noise temperatures of order 2 K have been achieved at frequencies below 2 GHz. Note also that these amplifiers may be expected to have very low $1/f$ gain noise, which should reduce the need to apply other techniques for measuring and compensating the amplifier's gain fluctuations.

Another route is to reduce the resonator frequency noise. It has recently been demonstrated[6, 37, 38]

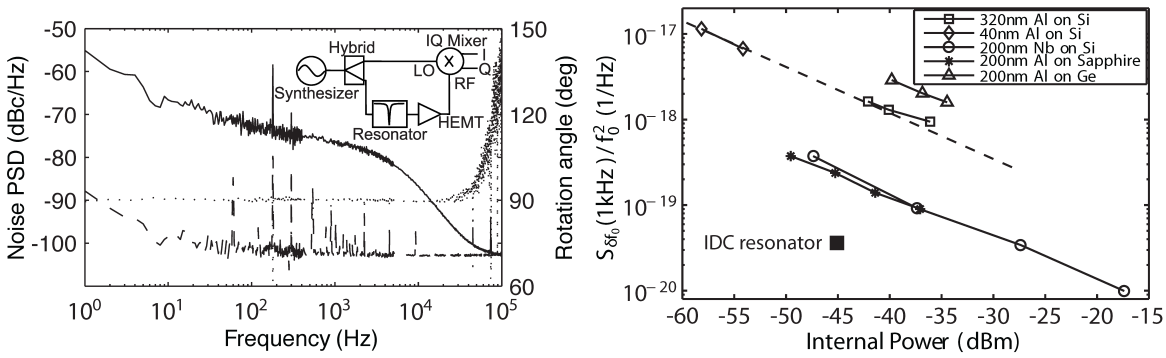

Figure 4: **Left**: An example[7, Fig. 2] of the measured noise power spectra for frequency readout (solid line) and dissipation readout (dashed line). The dotted line indicates the rotation angle between the direction of minimum noise and the tangent to the resonance circle; a value of 90 degrees indicates that the noise is essentially entirely due to frequency noise. Significant excess frequency noise is seen, whereas the noise floor for the dissipation readout is set by the cryogenic HEMT amplifier. The quality of the noise spectra below 10 Hz are limited by insufficient integration time but may be showing $1/f$ amplifier fluctuations; if necessary, such fluctuations can be removed using a variety of techniques, or possibly by using SiGe bipolar amplifiers with low $1/f$ noise. The frequency noise shows a $1/f^{0.5}$ slope in the 10 Hz to 10 kHz range; the corresponding NEP varies as $1/f^{0.25}$. The inset shows the usual homodyne readout scheme. **Right**: This plot [7, Fig. 3] shows the typical range of fractional frequency noise measured for CPW resonators. The frequency noise exhibits a $P^{-1/2}$ dependence on the microwave readout power. The square point represents very recent results using a new resonator design[32] that incorporates an interdigitated capacitor (IDC).

that the noise almost certainly originates primarily from a layer on the surface of the device. This surface layer contains two-level defects such as are commonly found in amorphous dielectric materials, and the fluctuation of these two-level systems (TLS) introduces noise in the resonator due to coupling of the TLS electric dipole moments to the resonator's electric field. A semi-empirical, quantitative theory of this noise mechanism has been developed[38] in which the TLS noise contribution scales as the cube of the electric field, $|E|^3$, and therefore those TLS located near the open-circuit end of the resonator are the most harmful. This insight has been used to develop a modified resonator geometry, in which the high-field "capacitive" portion of the CPW resonator is replaced by an interdigitated capacitor (IDC) structure with $10 - 20$ μm electrode spacing, as compared to the 2 μm spacing used for the CPW line. Recent measurements[32] show that this new IDC design has dramatically lower noise (see Fig. 4), currently by about a factor of 10 in terms of the frequency noise power spectrum, corresponding to a factor of $\sqrt{10}$ in NEP. These results confirm essential aspects of the noise model and again show that the noise really is not related to the superconductor. Further significant noise reductions may be expected in the future as the insights offered by the new noise model are more fully exploited.

2 State of Maturity

A small camera was built and taken to the Caltech Submillimeter Observatory (CSO) in March 2007 in order to demonstrate the technology.[5, 39] The camera was based on a 4×4, dual-band detector array as illustrated in Figures 5 and 6. The array chip was mounted into a simple housing (Fig. 7) and installed into a cryostat containing the optics and a 250 mK ^{3}He/^{3}He/^{4}He refrigerator. The frequency response was measured in the laboratory using a Fourier-transform spectrometer, which confirmed dual-band operation with the desired bandpasses (Fig. 7). The beam patterns were also measured in the laboratory and were found to generally agree with expectations. Using a digital readout system based on commercially available hardware[40], successful astronomical observations of bright objects (planets, HII regions) were made at the CSO, which again demonstrated the basic functionality of the system.

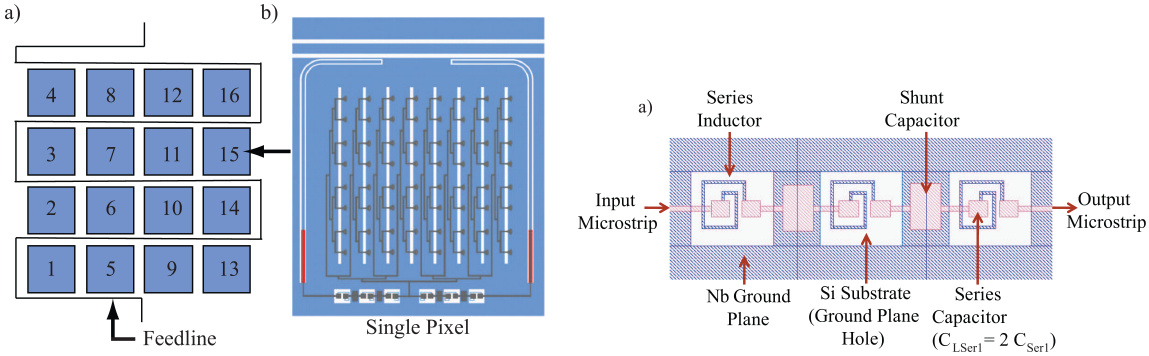

Figure 5: **Left**: The layout of a 4×4 array of dual-band pixels. Each pixel consists of a multislot antenna and an in-phase binary combining network; two on-chip filters that define the two bands centered at 230 GHz and 340 GHz; and two Nb/Al hybrid CPW resonators that serve as the detectors for the two bands. A common feedline is meandered past each pixel in the 4×4 array and simultaneously reads out all 32 detectors. **Right**: A close-up of the mm-wave bandpass filter design. The filter is a lumped-element design using spiral series inductors, and both series and shunt parallel-plate capacitors

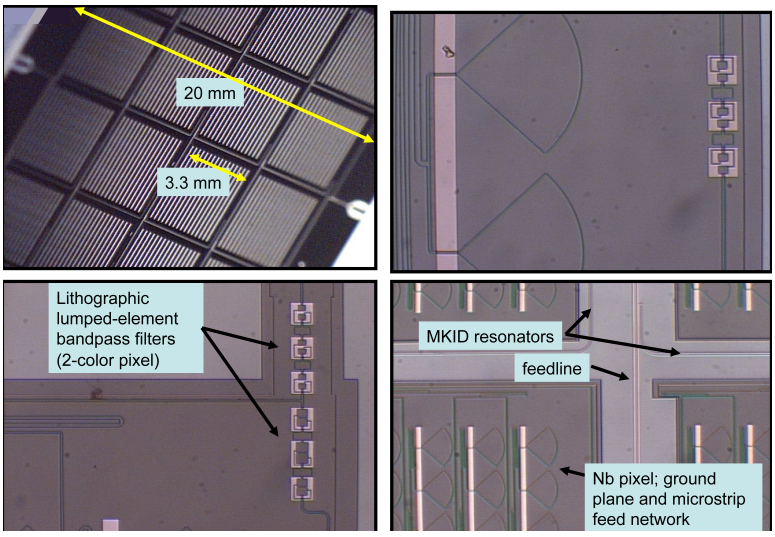

Figure 6: Microscope photographs of the 4×4 dual-band array. Each pixel is ~ 3.3 mm square. Microstrip radial stubs acting as mm-wave short circuits are used to couple the microstrip in-phase combining network to the slot antennas.

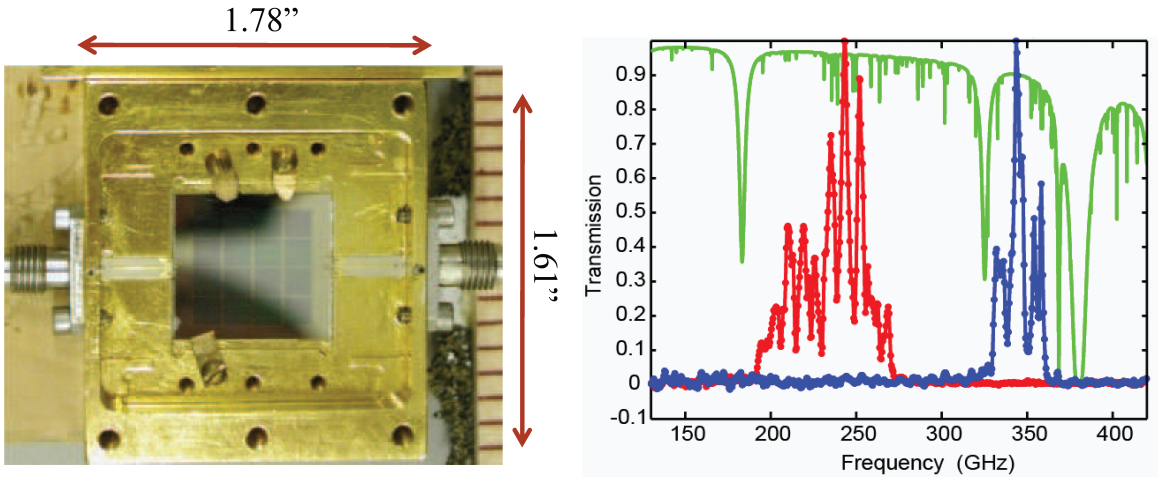

Figure 7: **Left**: The 4×4 array chip is mounted in a simple metal box. The input and output connections are wire-bonded to CPW to microstrip transitions fabricated on circuit boards, which are soldered to the center pins of the SMA/K coaxial connectors. **Right**: The frequency responses measured for a single dual-band pixel, indicating good agreement with the design values of the turn-on and turn-off frequencies of the on-chip filters. The lack of anti-reflection coatings on some of the optics may be causing the observed fringes; additional measurements are in progress.

This quick ($\sim$ 6 month) exercise proved highly useful and revealed a number of significant issues. The resonators were found to be highly sensitive to the Earth's magnetic field, and this had a serious impact on the sensitivity achieved. A proper magnetic shield was subsequently designed and manufactured, and will be implemented for the next telescope demonstration. The physics of this effect is currently being investigated[41]; simple modifications to the resonator design may substantially reduce their magnetic field sensitivity. In addition, we have found that small field variations only affect the resonance frequency, so the problem could be circumvented using dissipation readout. A second issue was that the devices were found to be substantially overcoupled ($Q_c >> Q_i$), which again adversely impacts the sensitivity. This situation is now being investigated in detail and the lessons learned will be applied to the next version of the array design.

In order to verify the basic optical efficiency of the devices, measurements were performed in a laboratory dilution refrigerator cryostat containing a cryogenic blackbody. This setup has the advantage of having minimal optics between the detector and the source, and also has minimum levels of stray light. These results indicate that the overall efficiency is rather high, of order $\sim 50\%$.

The present situation can be summarized by saying that essentially all aspects of the basic physics of the detector operation have been confirmed and match expectations. In addition, a fully-functional detector array incorporating antennas and on-chip filters has been demonstrated. However, the operation of a fully optimized array at the expected sensitivity in a complete system capable of astronomical observations is still a work in progress - we expect to reach this milestone in about a years' time

A much larger camera consisting of a 24×24 array of four-band pixels is now under construction (NSF ATI) for the CSO and is expected to be completed in mid-2010. One of the major tasks is the implementation of the 2304-channel readout electronics. We have studied the technical requirements in detail and have produced a specifications document. Our requirements are well within the state of the art, and we are currently in discussions with potential vendors for the development of a turnkey system.

3 Advantages and Disadvantages

The primary advantage of superconducting microresonator detectors is the relatively low cost for implementing a full system. This is due to several factors:

- Detector fabrication is very straightforward and fast, requiring only 3-6 levels of lithography depending on the design, and yields are high. Critical temperature (T_c) uniformity is not a significant issue. Film thickness uniformity is necessary at the $\sim 10\%$ level.
- The devices are already fully multiplexed and a separate complex multiplexer chip is not needed. In addition, procedures for attaching the detector array to a multiplexer array (using wire bonding, indium bump bonding, etc.) are not required.
- Compared to first-generation TDM/FDM SQUID multiplexing, much larger multiplexing factors ($\sim 10^3$ instead of $\sim 10^1$) are possible. This reduces the wire count dramatically.
- Microresonator detectors can be used as "drop-in" replacements for microstrip-coupled TES bolometers. This allows existing antenna designs, filter designs, etc. to be reused.

There are also several technical advantages. Perhaps the most useful is that the saturation characteristics are very benign. As the optical load is increased, the internal quality factor Q_i drops, and eventually no longer obeys the optimal coupling condition $Q_c = Q_i$. This just causes the amplifier noise contribution to increase - the detector remains functional with a graceful degradation of its performance. Another advantage is speed: leg-isolated bolometers will be several orders of magnitude slower for the same NEP. The low cost and ease of implementation also facilitates rapid development of the technology. Finally, superconducting microresonators are finding numerous applications in other areas of physics, and the research community in this area is growing rapidly.

The primary disadvantages are:

- Lower level of maturity. TES bolometer development has a $\sim$ 5-year head start.
- Sensitivity. Using dissipation readout and commonly available HEMT amplifiers, sensitivities around $2\times$ BLIP are achievable today, and somewhat better using state-of-the-art SiGe amplifiers. Comparable performance levels should also be possible with frequency readout along with emerging low-noise resonator designs. Reaching BLIP-level performance should eventually be possible but will likely take several more years of effort.
- Readout electronics are not yet available. A first-generation, 2k-channel FPGA-based readout electronics system should be ready by mid-2010. A low power dissipation readout system suitable for space will likely require eventual development of a custom ASIC; however this is best done after the signal processing schemes have been developed and demonstrated using FPGAs.

4 Technology Readiness Level

I judge the level to be around TRL4: a "low-fidelity" demonstration of a working system has been achieved (the demonstration camera on the CSO). I expect the TRL level to jump to 5-6 over the next several years; the milestone will be having the new large CSO camera working at its target performance. Prior to inclusion in a CMBpol mission proposal, one would also like to demonstrate dual-polarization versions working at the desired sensitivity levels in the laboratory.

References

[1] P. K. Day, H. G. LeDuc, B. A. Mazin, A. Vayonakis, and J. Zmuidzinas, "A broadband superconducting detector suitable for use in large arrays," *Nature*, vol. 425, no. 6960, pp. 817–821, October 2003.

[2] B. A. Mazin, P. K. Day, J. Zmuidzinas, and H. G. LeDuc, "Multiplexable kinetic inductance detectors," *AIP Conference Proceedings*, no. 605, pp. 309–312, 2002.

[3] B. A. Mazin, P. K. Day, H. G. LeDuc, A. Vayonakis, and J. Zmuidzinas, "Superconducting kinetic inductance photon detectors," *Proceedings of the SPIE - The International Society for Optical Engineering*, vol. 4849, pp. 283–293, 2002.

[4] B. A. Mazin, "Microwave kinetic inductance detectors," Ph.D. dissertation, California Institute of Technology, Pasadena, CA 91125, August 2004.

[5] S. Kumar, "Submillimeter wave camera using a novel photon detector technology," Ph.D. dissertation, California Institute of Technology, Pasadena, CA 91125, 2008.

[6] J. Gao, "The physics of superconducting microwave resonators," Ph.D. dissertation, California Institute of Technology, Pasadena, CA 91125, 2008.

[7] J. S. Gao, J. Zmuidzinas, B. A. Mazin, H. G. LeDuc, and P. K. Day, "Noise properties of superconducting coplanar waveguide microwave resonators," *Applied Physics Letters*, vol. 90, no. 10, p. 102507, Mar 2007.

[8] J. Gao, J. Zmuidzinas, A. Vayonakis, P. Day, B. Mazin, and H. Leduc, "Equivalence of the effects on the complex conductivity of superconductor due to temperature change and external pair breaking," *Journal of Low Temperature Physics*, vol. 151, no. 1-2, pp. 557–563, April 2008.

[9] A. D. O'Connell, M. Ansmann, R. C. Bialczak, M. Hofheinz, N. Katz, E. Lucero, C. McKenney, M. Neeley, H. Wang, E. M. Weig, A. N. Cleland, and J. M. Martinis, "Microwave dielectric loss at single photon energies and millikelvin temperatures," *Applied Physics Letters*, vol. 92, no. 11, March 2008.

[10] J. J. Bock, A. Goldin, C. Hunt, A. E. Lange, H. G. LeDuc, P. K. Day, A. Vayonakis, and J. Zmuidzinas, "Integrated focal plane arrays for millimeter-wave astronomy," *AIP Conference Proceedings*, no. 605, pp. 243–246, 2002.

[11] A. Goldin, J. J. Bock, C. Hunt, A. E. Lange, H. LeDuc, A. Vayonakis, and J. Zmuidzinas, "SAMBA: superconducting antenna-coupled, multi-frequency, bolometric array," *AIP Conference Proceedings*, no. 605, pp. 251–254, 2002.

[12] A. Goldin, J. J. Bock, C. L. Hunt, A. E. Lange, H. G. LeDuc, A. Vayonakis, and J. Zmuidzinas, "Design of broadband filters and antennas for SAMBA," *Proceedings of the SPIE - The International Society for Optical Engineering*, vol. 4855, pp. 163–171, 2003.

[13] A. Goldin, J. J. Bock, A. E. Lange, H. LeDuc, A. Vayonakis, and J. Zmuidzinas, "Antennas for bolometric focal plane," *Nucl. Instrum. Meth. Phys. Res. A*, vol. 520, no. 1-3, pp. 390–392, March 2004.

[14] P. K. Day, H. G. Leduc, A. Goldin, T. Vayonakis, B. A. Mazin, S. Kumar, J. Gao, and J. Zmuidzinas, "Antenna-coupled microwave kinetic inductance detectors," *Nucl. Instrum. Meth. Phys. Res. A*, vol. 559, no. 2, pp. 561–563, Apr 2006.

[15] C. L. Kuo, P. Ade, J. J. Bock, P. Day, A. Goldin, S. Golwala, M. Halpern, G. Hilton, W. Holmes, V. Hristov, K. Irwin, W. C. Jones, M. Kenyon, A. E. Lange, H. G. LeDuc, C. MacTavish, T. Montroy, C. B. Netterfield, P. Rossinot, J. Ruhl, A. Vayonakis, G. Wang, M. Yun, and J. Zmuidzinas, "Antenna-coupled tes bolometers for the SPIDER experiment," *Nucl. Instrum. Meth. Phys. Res. A*, vol. 559, no. 2, pp. 608–610, Apr 2006.

[16] G. Chattopadhyay, C.-L. Kuo, P. Day, J. J. Bock, J. Zmuidzinas, and A. E. Lange, "Planar antenna arrays for CMB polarization detection," in *Proc. 2007 Joint 32nd International Conference on Infrared and Millimeter Waves and the 15th International Conference on Terahertz Electronics (IRMMW-THz)*, 2008, pp. 184–185.

[17] C. L. Hunt, J. J. Bock, P. K. Day, A. Goldin, A. E. Lange, H. G. LeDuc, A. Vayonakis, and J. Zmuidzinas, "Transition-edge superconducting antenna-coupled bolometer," *Proceedings of the SPIE - The International Society for Optical Engineering*, vol. 4855, pp. 318–321, 2003.

[18] M. Myers, W. Holzapfel, A. Lee, R. O'Brient, P. Richards, H. Tran, P. Ade, G. Engargiola, A. Smith, and H. Spieler, "An antenna-coupled bolometer with an integrated microstrip bandpass filter," *Applied Physics Letters*, vol. 86, no. 11, March 2005.

[19] M. Myers, P. Ade, G. Engargiola, W. Holzapfel, A. Lee, R. O'Brient, P. Richards, A. Smith, H. Spieler, and H. Tran, "Antenna-coupled bolometers for millimeter waves," *IEEE Transactions On Applied Superconductivity*, vol. 15, no. 2, pp. 564–566, June 2005.

[20] M. Myers, A. Peter, K. Arnold, G. Engargiola, B. Holzapfel, A. Lee, R. O'Brient, P. Richards, A. Smith, H. Spieler, and T. Huan, "Antenna-coupled bolometer arrays using transition-edge sensors," *Nucl. Instrum. Meth. Phys. Res. A*, vol. 559, no. 2, pp. 531–533, April 2006.

[21] M. J. Myers, K. Arnold, P. Ade, G. Engargiola, W. Holzapfel, A. T. Lee, X. Meng, R. O'Brient, P. L. Richards, H. Spieler, and H. T. Tran, "Antenna-coupled bolometer arrays for measurement of the cosmic microwave background polarization," *Journal of Low Temperature Physics*, vol. 151, no. 1-2, pp. 464–470, April 2008.

[22] R. O'Brient, P. A. R. Ade, K. Arnold, G. Engargiola, W. Holzapfel, A. T. Lee, M. J. Myers, X. F. Meng, E. Quealy, P. L. Richards, H. Spieler, and H. T. Tran, "A multi-band dual-polarized antenna-coupled tes bolometer," *Journal of Low Temperature Physics*, vol. 151, no. 1-2, pp. 459–463, April 2008.

[23] J. W. Kooi, G. Chattopadhyay, S. Withington, F. Rice, J. Zmuidzinas, C. Walker, and G. Yassin, "A full-height waveguide to thin-film microstrip transition with exceptional rf bandwidth and coupling efficiency," *Int. J. IR and MM Waves*, vol. 24, no. 3, pp. 261–284, March 2003.

[24] T. Stevenson, W. Hsieh, G. Schneider, D. Travers, N. Cao, E. Wollack, M. Limon, and A. Kogut, "Building blocks for a polarimeter-on-a-chip," *Nucl. Instrum. Meth. Phys. Res. A*, vol. 559, no. 2, pp. 611–613, April 2006.

[25] D. M. Glowacka, D. J. Goldie, S. Withington, M. Crane, V. Tsaneva, M. D. Audley, and A. Bunting, "A fabrication process for microstrip-coupled superconducting transition edge sensors giving highly reproducible device characteristics," *Journal of Low Temperature Physics*, vol. 151, no. 1-2, pp. 249–254, April 2008.

[26] D. J. Goldie, M. D. Audley, D. M. Glowacka, V. N. Tsaneva, and S. Withington, "Transition edge sensors for bolometric applications: responsivity and saturation," *Journal of Applied Physics*, vol. 103, no. 8, April 2008.

[27] T. Stevenson, D. Benford, C. Bennett, N. Cao, D. Chuss, K. Denis, W. Hsieh, A. Kogut, S. Moseley, J. Panek, G. Schneider, D. Travers, K. U-Yen, G. Voellmer, and E. Wollack, "Cosmic microwave background polarization detector with high efficiency, broad bandwidth, and highly symmetric coupling to transition edge sensor bolometers," *Journal of Low Temperature Physics*, vol. 151, no. 1-2, pp. 471–476, April 2008.

[28] S. J. C. Yates, J. J. A. Baselmans, R. Barends, Y. Lankwarden, H. F. Hoevers, J. Gao, T. Klapwijk, A. Neto, D. J. Bekers, G. Gerini, S. Doyle, P. D. Mauskopf, and P. Ade, "Antenna coupled kinetic inductance detectors for space based sub-mm astronomy," 2008, presented at the 2nd Workshop on the Physics and Applications of Superconducting Microresonators.

[29] S. Doyle, P. Mauskopf, J. Naylon, A. Porch, and C. Duncombe, "Lumped element kinetic inductance detectors," *Journal of Low Temperature Physics*, vol. 151, no. 1-2, pp. 530–536, April 2008.

[30] S. Doyle, "Kinetic inductance detectors," Ph.D. dissertation, Cardiff University, 2008.

[31] R. Barends, J. J. A. Baselmans, S. J. C. Yates, J. R. Gao, J. N. Hovenier, and T. M. Klapwijk, "Quasiparticle relaxation in optically excited high-Q superconducting resonators," *Physical Review Letters*, vol. 100, no. 25, June 2008.

[32] O. Noroozian, P. Day, J.-S. Gao, J. Glenn, S. Golwala, H. LeDuc, P.Maloney, B. Mazin, J. Sayers, J. Schlaerth, A. Vayonakis, and J.Zmuidzinas, "New resonator designs for reduced frequency noise in microwave kinetic inductance detectors (MKID)," 2008, presented at the 2nd Workshop on the Physics and Applications of Superconducting Microresonators.

[33] J. Baselmans, S. J. C. Yates, R. Barends, Y. J. Y. Lankwarden, J. R. Gao, H. Hoevers, and T. M. Klapwijk, "Noise and sensitivity of aluminum kinetic inductance detectors for sub-mm astronomy," *Journal of Low Temperature Physics*, vol. 151, no. 1-2, pp. 524–529, April 2008.

[34] J. Baselmans, S. Yates, R. Barends, J.-J. Lankwarden, J. Gao, H. F. Hoevers, and T. Klapwijk, "Optimizing kinetic inductance detectors for low background applications," June 19-20 2008, presented at the 2nd Workshop on the Physics and Applications of Superconducting Microresonators, SRON Utrecht.

[35] S. Weinreb, J. C. Bardin, and H. Mani, "Design of cryogenic SiGe low-noise amplifiers," *IEEE Transactions On Microwave Theory and Techniques*, vol. 55, no. 11, pp. 2306–2312, November 2007.

[36] T. K. Thrivikraman, J. Yuan, J. C. Bardin, H. Mani, S. D. Phillips, W.-M. L. Kuo, J. D. Cressler, and S. Weinreb, "SiGe HBT X-band LNAs for ultra-low-noise cryogenic receivers," *IEEE Microwave and Wireless Components Letters*, vol. 18, no. 7, pp. 476–478, July 2008.

[37] J. Gao, M. Daal, A. Vayonakis, S. Kumar, J. Zmuidzinas, B. Sadoulet, B. A. Mazin, P. K. Day, and H. G. Leduc, "Experimental evidence for a surface distribution of two-level systems in superconducting lithographed microwave resonators," *Applied Physics Letters*, vol. 92, no. 15, April 2008.

[38] J. Gao, M. Daal, J. M. Martinis, A. Vayonakis, J. Zmuidzinas, B. Sadoulet, B. A. Mazin, P. K. Day, and H. G. Leduc, "A semiempirical model for two-level system noise in superconducting microresonators," *Applied Physics Letters*, vol. 92, no. 21, May 2008.

[39] J. Schlaerth, A. Vayonakis, P. Day, J. Glenn, J. Gao, S. Golwala, S. Kumar, H. LeDuc, B. Mazin, J. Vaillancourt, and J. Zmuidzinas, "A millimeter and submillimeter kinetic inductance detector camera," *Journal of Low Temperature Physics*, vol. 151, no. 3-4, pp. 684–689, May 2008.

[40] B. A. Mazin, P. K. Day, K. D. Irwin, C. D. Reintsema, and J. Zmuidzinas, "Digital readouts for large microwave low-temperature detector arrays," *Nucl. Instrum. Meth. Phys. Res. A*, vol. 559, no. 2, pp. 799–801, April 2006.

[41] C. Muirhead, J. Healey, and M. Colclough, "Magnetic field tuning of coplanar waveguide resonators," 2008, presented at the 2nd Workshop on the Physics and Applications of Superconducting Microresonators.